



Flavour Prospect at Future Circular Colliders (Focused on FCC-ee and $B_c \rightarrow \tau \nu$ ($\tau \rightarrow 3\pi \nu$))

HQL conference 2021

September 17, 2021
Clement Helsens, CERN-EP

Flavour Physics at FCC-ee: Brief Overview



- Strong case for flavour physics at the Z^0 - pole at FCC-ee
- Production of up to 5×10^{12} Z^0 's anticipated with 4 IPs (CEPC ~ 10 times less)
 - 7.6×10^{11} bb
 - 6.1×10^{11} cc
 - 1.7×10^{11} $\tau\tau$
- Z^0 production rate of ~ 100 kHz and clean e^+e^- environment allows triggerless readout
 - No efficiency losses from online selection cuts
- We must identify the physics cases where FCC-ee can perform better than either LHCb Upgrade II or Belle II

Goals

Medium-term

- Enable informed detector design studies with a focus on flavour phys. at FCC-ee
 - What detector specifications are vital, and which are desirable
 - Does heavy flavour favor a particular bunch structure?

Shorter-term

- Identify highest-priority heavy-flavour modes for FCC-ee
 - How can FCC-ee extend physics reach beyond LCHb and Belle-II?
 - What modes are the most theoretically compelling?

Immediate

- Develop common software tools in FCCSW to facilitate studies
 - Interface EvtGen, MC-truth matching, Particle combination to reconstruct modes of interest
 - Reconstruction/analysis tools (flavour tagging, decay chain building, vertex fitting, etc...)

Species Yields at FCC-ee (per IP per year)



- Production fractions from $e^+e^- \rightarrow Z^0 \rightarrow ff$
- No efficiency factors from reconstruction or selection included

Z^0 mode	Species	Production fraction	Yield
bb	B^\pm	0.43	4.9×10^{10}
bb	B^0	0.43	4.9×10^{10}
bb	B_s^0	0.098	1.1×10^{10}
bb	B_c^\pm	4×10^{-4}	4.5×10^7
$\tau\tau$	τ	1	2.5×10^{10}
cc	D^\pm	0.43	3.9×10^{10}

Examples: Fully rec. modes with charged tracks



- $B^0 \rightarrow (K^{*0} \rightarrow K\pi)e^+e^-$
 - Rare decay involving $b \rightarrow s$ transition ($B = 3.4 \times 10^{-7}$), sensitive to NP in loop-level processes
 - Measurement of electron mode challenging at LHCb - Expect $\sim 140k$ events with 4 IPs
- $B^0 \rightarrow \mu^+\mu^-$
 - Very rare decay (in SM $B = 1.07 \times 10^{-10}$) which is sensitive to NP contributions
 - Well motivated for observation and $< 10\%$ B precision - Expect ~ 80 events with 4 IPs
- $Bs^0 \rightarrow (Ds^- \rightarrow K^+K^-\pi^-)K^+$
 - Time dependent CP violation due to interference between mix. and dec. amplitudes
 - Interesting for FCC-ee because Belle-II does not resolve Bs^0 time-dependence, LHCb flavour tagging is poor - Expect ~ 2 millions events with 4 IPs

Examples: Fully rec. modes with neutrals



- $\tau^+ \rightarrow \mu^+ \gamma$
 - Lepton flavour violating decay with unobservable rate in SM, best limit $B < 4.4 \times 10^{-8}$
 - Challenging due to lack of τ vertex and presence of photon
 - With 4 IPs, observation likely possible at $B = 6 \times 10^{-11}$, Belle-II projection is 10^{-9}
- $B_s^0 \rightarrow (\phi \rightarrow K^+ K^-) \gamma$
 - Decay involves $b \rightarrow s \gamma$ loop-level transition. Photon polarisation sensitive to NP
 - Polarisation observable $A^\Delta(\text{SM}) = 0.047 + 0.029 - 0.025$
 - Anticipate ~ 3 million events with 4 IPs, precision below theory error on A^Δ possible
- $D^+ \rightarrow \pi^+ \pi^0$
 - In SM, decay dominated by two singly Cabibbo-suppressed tree-level diagrams
 - No CP asymmetry expected in SM \rightarrow measuring CP asymmetry clear sign of NP!
 - $\sim 5 \times 10^{-5}$ precision on A_{CP} could be achieved if systematics can be controlled

Examples: Modes with missing momentum

- $B^0 \rightarrow K^{*0} \tau^+ \tau^-$
 - Tauonic equivalent of $K^{*0} l^+ l^-$, critical to extend the $b \rightarrow sll$ lepton universality picture
 - Total $B=3.2 \times 10^{-10}$ assuming B^0 decay $B=10^{-7}$ and reconstruct only $K^* \rightarrow K\pi$ and $\tau \rightarrow 3\pi\nu$
 - $(4.9 \times 10^{10}) \times (3.2 \times 10^{-10}) = 16$ events per IP per year (sub-decays with neutrals can boost $\sim 10^3$)

- $B_s^0 \rightarrow \tau^+ \tau^-$
 - Not yet observed, with only weak B limits $\sim 10^{-2}$, Significant NP enhancement (larger m_τ)
 - With SM $B \sim 10^{-6}$, and $\tau \rightarrow 3\pi\nu$, 80 events per IP per year

- $B_c^+ \rightarrow \tau^+ \nu_\tau$ (no chance a LHCb, no B_c^+ at Belle II)
 - Same vertex factor as $B^0 \rightarrow D^{(*)} \tau \nu_\tau$, important crosscheck of $b \rightarrow c l \nu$ lepton univer. meas.
 - With SM, $B \sim 2.5\%$ and $\tau \rightarrow 3\pi\nu$, 100 000 events per experiment per year
 - Next slides will focus on this channel

$Bc^+ \rightarrow \tau^+ \nu_\tau$ ($\tau \rightarrow 3\pi\nu$) prospects at FCC-ee

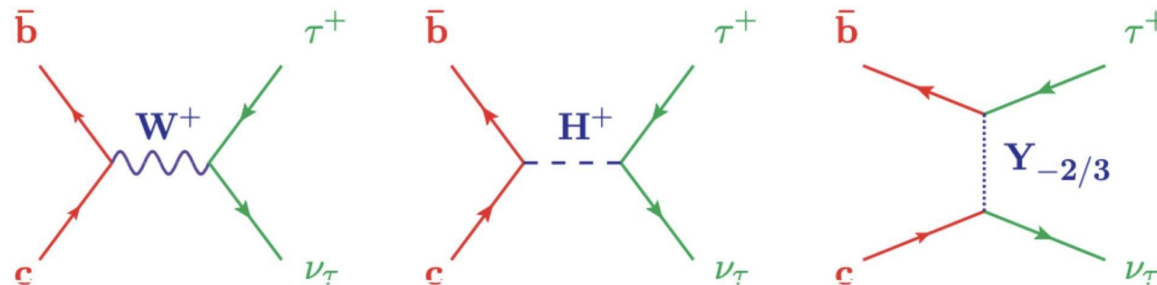


<https://arxiv.org/abs/2105.13330>

Submitted to JHEP

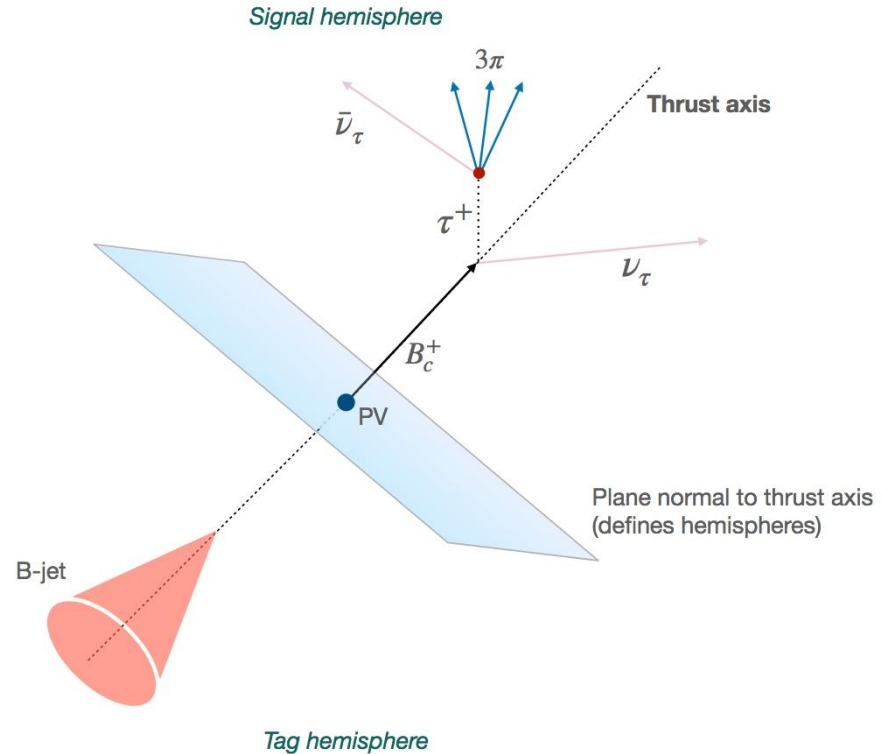
Motivation

- $B_c \rightarrow \tau \nu_\tau$ is a unique flavour opportunity at FCC-ee
 - Not possible at LHCb due to missing energy, lack of constraints and reconstructed info.
 - No B_c mesons produced at Belle II
- Involves the same Feynman vertex factors as $b \rightarrow c \tau \nu_\tau$ decays
 - Measurements of $R(D)$ and $R(D^*)$ show a $\sim 3\text{-}4\sigma$ tension with the Standard Model
 - Measuring $B(B_c \rightarrow \tau \nu_\tau)$ would provide an independent test of lepton universality and yield strong constraints on possible new physics explanations
 - $B(B_c \rightarrow \tau \nu_\tau)$ SM = $(1.94 \pm 0.09) \%$



Event topology for $B_c^+ \rightarrow \tau^+ \nu_\tau$

- Reconstruction of the thrust axis
 - used to define in which hemisphere the particles fall in
- Large missing energy,
 - 2 neutrinos in the signal decay
 - 2 hemisphere have rather different energy distributions



Using $\tau^- \rightarrow \pi^+ \pi^- \pi^- \nu_\tau$

- Existing feasibility study for CEPC (arxiv:2007.08234)
 - Using leptonic electron and muon tau decays
- Using tree-prong hadronic mode for this work
 - Provides τ decay vertex, and thus a measure of combined Bc and τ flight
 - Branching fraction of 9% provides sufficient decay rate
- Reject background from $Z \rightarrow bb/cc/qq$ using
 - Event level energy properties
 - Properties of the reconstructed 3π candidate
 - Two stage MVA approach

Samples and Software

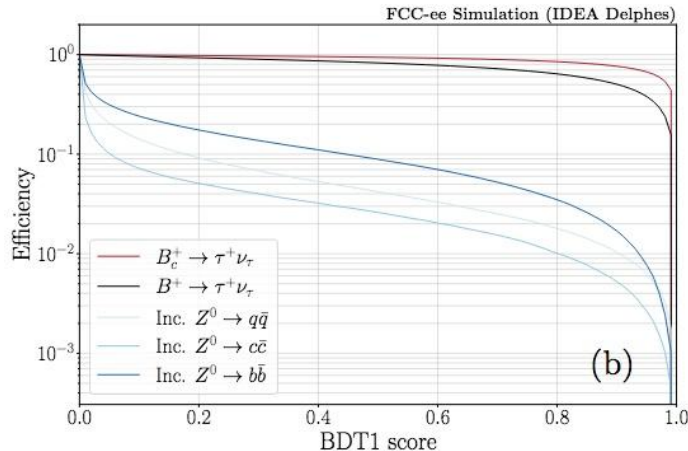
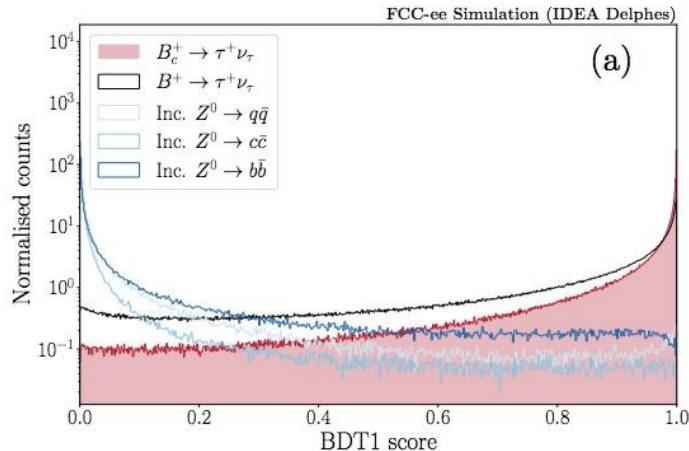


- Using official FCC-ee production ([see here](#))
 - 10^6 signal events with $\tau^- \rightarrow \pi^+ \pi^- \pi^- \nu_\tau$ generated with EvtGen
 - 10^9 events Zbb/cc/qq with Pythia8
 - Samples of exclusive B hadron background decays generated to study selection efficiency more accurately 200×10^6 per decay times 28 species
 - Dedicated orthogonal production of 10^9 events for MVA training ([see here](#))

- First published result using common software
 - Events generated with [key4Hep](#) software stack in the [EDM4Hep](#) data format
 - EDM4Hep events processed with [FCCAnalyses](#) to produce “flat ntuples”
 - Set of [custom Python analysis tools](#) to process the “flat ntuples” and produce results

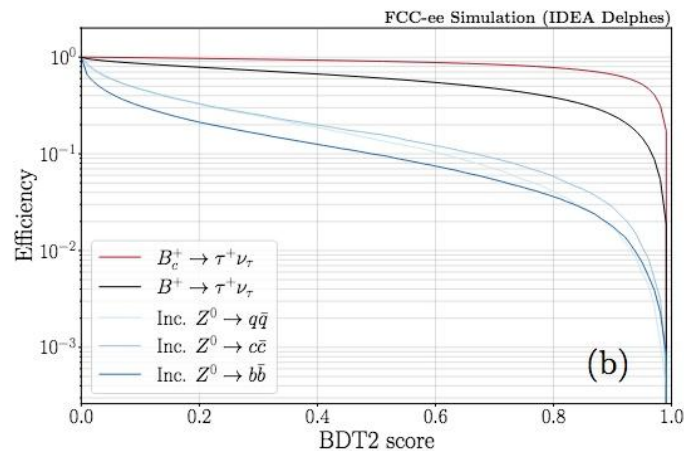
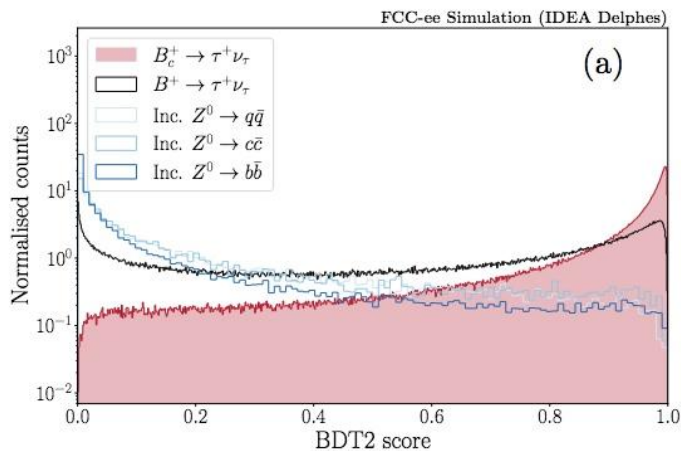
First stage MVA performance

- Strong rejection of all three backgrounds with ROC = 0.984
 - $Z \rightarrow bb$ rejected less since it produces most missing energy
- $B^+ \rightarrow \tau^+ \nu_\tau$ also rejected to an extent (different event-level prop. compared to Bc^+)
 - Important background, enhanced 1000x due to B^+ vs. Bc^+ production rate, but lower due to CKM suppression ($|V_{ub}|^2$ vs. $|V_{cb}|^2$)
 - Expect 5 times more $B^+ \rightarrow \tau^+ \nu_\tau$ than signal before any cuts



Second stage MVA performance

- All backgrounds rejected very well, with ROC = 0.966
- Excellent rejection of $B^+ \rightarrow \tau^+ \nu_\tau$ mode as well, even if it is not used in the training
 - B^+ mode reduced to a level where it must be constrained from indep. measurements
 - Described more in toy fit setup later



2D MVA cut optimisation

- Tune the two MVA cuts to maximise purity of signal $S/(S+B)$ to enable a precise $B(Bc^+ \rightarrow \tau^+ \nu_\tau)$ measurement
 - Estimate S and B expected from 5×10^{12} Z at FCC-ee
- Inclusive $Z \rightarrow cc/qq$ rejected at 10^9 level with sufficiently tight MVA cuts
 - All generated events are rejected
 - Do not consider these in subsequent studies
- Inclusive $Z \rightarrow bb$ statistics are insufficient to assess background rejection to a high enough level or create fit templates
 - Generate a set of exclusive B^0 , B^+ , B_s^0 and Λb^0 modes where all B-hadrons decay products are decayed inclusively
 - Focus on modes where a τ or charm hadron produces a displaced 3π along with an other charm hadron

Cut optimisation - results

- Estimated yields with
 - $N_Z = 5 \times 10^{12}$, $B(Z \rightarrow bb) = 0.1512$
 - B hadron production fraction from Pythia

- Estimate signal yield using
 - $B(Bc^+ \rightarrow \tau^+ \nu_\tau) = 1.94\%$ (SM prediction)
 - $f_c = 0.0004$ from Pythia and selection efficiency from signal MC

- Estimate $B^+ \rightarrow \tau^+ \nu_\tau$ and exclusive B-hadron background yields using
 - PDG B's production fractions and MC efficiencies

- Best signal yields of 4295 events with 85% purity ($\varepsilon = 0.39\%$)

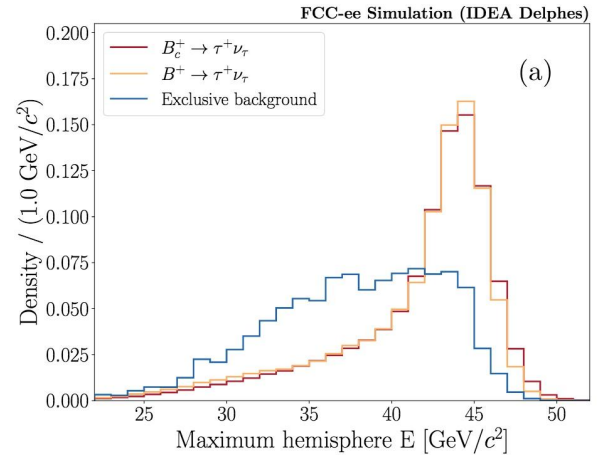
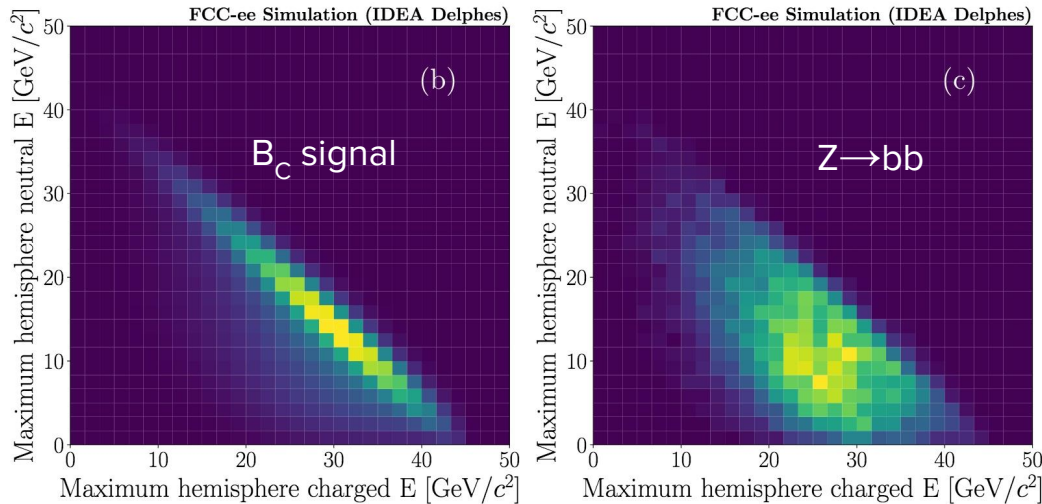
- 285 events expected for $B^+ \rightarrow \tau^+ \nu_\tau$ mode ($\varepsilon = 4.3 \times 10^{-5}$)

- Background level of 448 events estimated from sum of all exclusive modes, scaled by 2.5 (inclusive vs. exclusive ratio)

Signal vs. background discrimination for fit



- In an inclusive Zbb event, either side could have max. E
 - However, in a signal decay, the max. E hemis is most likely the non-signal side
 - In signal events, max. E hemisphere looks a lot like an inclusive decay peak near $m(Z)/2$
 - In BG, the selection req. bias this hemisphere down in energy, giving discrimination

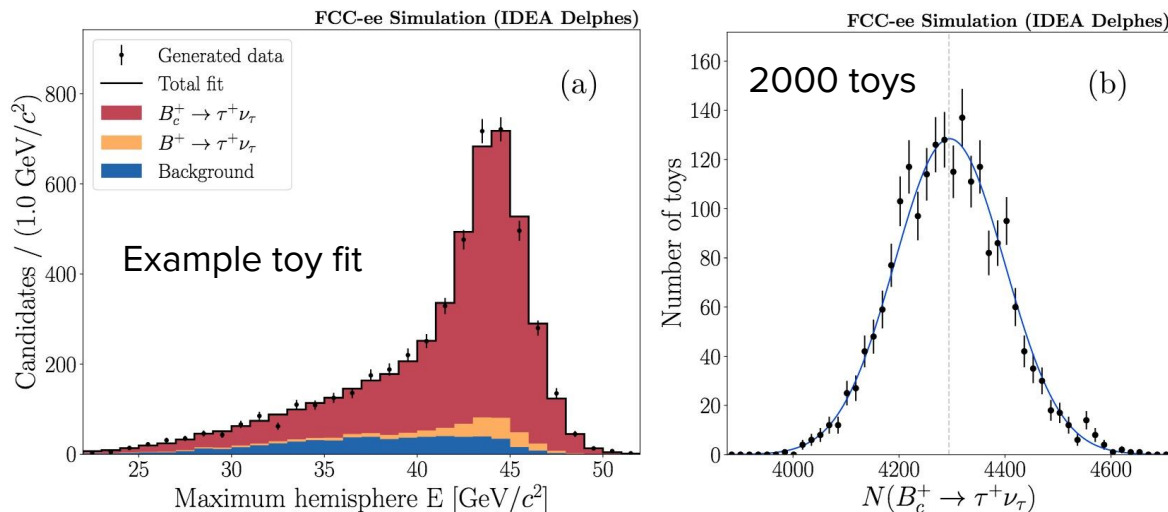


Toy Fit to Measure Signal Yield

- Energy of the maximum energy hemisphere used as the fit variable
- Create histogram templates in $Bc^+ \rightarrow \tau^+ \nu_\tau$, $B^+ \rightarrow \tau^+ \nu_\tau$, and exclusive (B^0 , B^+ , Bs^0 , Λb^0) background
 - Sum exclusive backgrounds according to their expected yields from the MVA cut opti.
- $B^+ \rightarrow \tau^+ \nu_\tau$ yield constrained in fit to the value found in the cut optimisation, with 5% relative uncertainty
 - Expected uncertainty on $B(B^+ \rightarrow \tau^+ \nu_\tau)$ from Belle II physics book
 - This mode contributes a yield of 5% relative to signal after all cuts, so the uncertainty from this is negligible

Toy Fit to Measure Signal Yield

- Toy dataset generated from a summed histogram PDF of signal, $B^+ \rightarrow \tau^+ \nu_\tau$ and total background, with yields as mentioned
 - Each bin is Poisson varied independently to create toys
- Signal and background yields vary freely in the toy fit - signal measured within 2.4%
 - Fit with 10x higher background level measures 2.9% uncertainty



Convert Signal Yields to $\mathcal{B}(B_c^+ \rightarrow \tau^+ \nu_\tau)$

$$R_c = \frac{\mathcal{B}(B_c^+ \rightarrow \tau^+ \nu_\tau)}{\mathcal{B}(B_c^+ \rightarrow J/\psi \mu^+ \nu_\mu)}$$

$$\mathcal{B}(B_c^+ \rightarrow \tau^+ \nu_\tau) = R_c \times \mathcal{B}(B_c^+ \rightarrow J/\psi \mu^+ \nu_\mu)^{\text{SM}}$$

$$= \frac{N(B_c^+ \rightarrow \tau^+ \nu_\tau)}{N(B_c^+ \rightarrow J/\psi \mu^+ \nu_\mu)} \times \frac{\epsilon(B_c^+ \rightarrow J/\psi \mu^+ \nu_\mu)}{\epsilon(B_c^+ \rightarrow \tau^+ \nu_\tau)} \times \frac{\mathcal{B}(J/\psi \rightarrow \mu^+ \mu^-)}{\mathcal{B}(\tau^+ \rightarrow \pi^+ \pi^+ \pi^- \bar{\nu}_\tau)}$$

- Signal yield measured in toy fit is based on an assumed $\mathcal{B}(B_c^+ \rightarrow \tau^+ \nu_\tau) = 1.94\%$
- Convert toy fit yield back to $\mathcal{B}(B_c^+ \rightarrow \tau^+ \nu_\tau)$ via correction factors, and assess the precision on branching ratio
- Use some external branching fractions as well as a theory prediction for $\mathcal{B}(B_c^+ \rightarrow J/\psi \mu^+ \nu_\mu) = 0.0135 \pm 0.0011$

$B(B_c^+ \rightarrow \tau^+ \nu_\tau)$ calculation input

- Expected signal yield from cut optimisation procedure
- Yield statistical uncertainty from toy fits, scaled up by $\sqrt{2}$ to account for potential systematics (template statistics, background modelling)
- Normalisation yield calculated in similar manner to signal, assuming fairly high efficiency for three-muon mode
 - Main loss due to $m(J/\psi\mu) > 5.3$ GeV cut needed to reject B^{+0} background, see 1407.2126

Term	Value	Explanation
$\epsilon(B_c^+ \rightarrow \tau^+ \nu_\tau)$	$(3.93 \pm 0.04) \times 10^{-3}$	From our MC (assume 1% precision)
$\epsilon(B_c^+ \rightarrow J/\psi\mu^+\nu_\mu)$	0.100 ± 0.001	Assume with 1% precision
$\mathcal{B}(J/\psi \rightarrow \mu\mu)$	$(5.96 \pm 0.03) \times 10^{-2}$	From PDG
$\mathcal{B}(\tau^+ \rightarrow 3\pi\nu_\tau)$	$(9.31 \pm 0.05) \times 10^{-2}$	From PDG
$N(B_c^+ \rightarrow \tau^+ \nu_\tau)$	4295 ± 146	Uses $N_{b\bar{b}}$, f_c , \mathcal{B} 's, and ϵ
$N(B_c^+ \rightarrow J/\psi\mu^+\nu_\mu)$	48670 ± 220	Uses $N_{b\bar{b}}$, f_c , \mathcal{B} 's, and ϵ
$\mathcal{B}(B_c^+ \rightarrow J/\psi\mu^+\nu_\mu)$	0.0135 ± 0.0011	Calculation from O. Sumensari

17

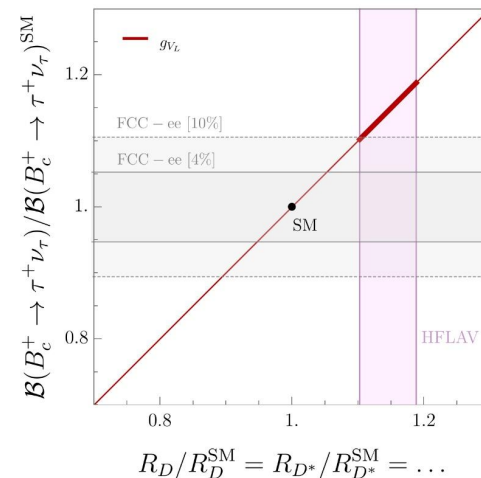
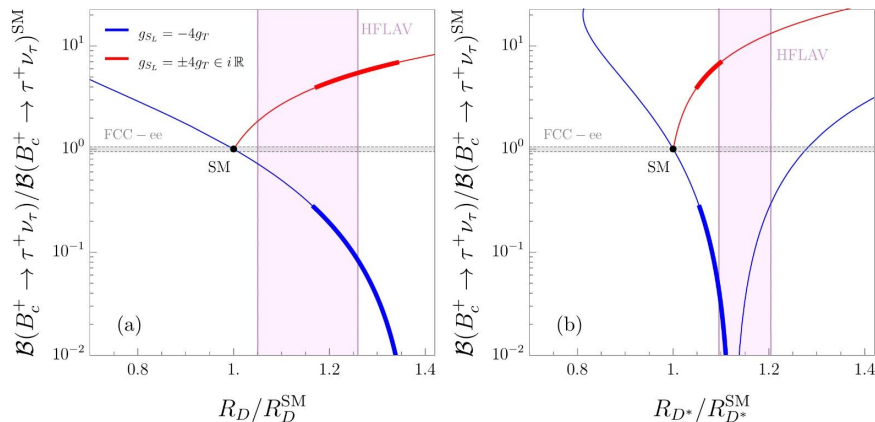
Anticipated precision on $B(Bc^+ \rightarrow \tau^+ \nu_\tau)$

$$B(Bc \rightarrow \tau \nu_\tau) = (1.941 \pm 0.175) \times 10^{-2}$$

- Recover the input branching ratio central value as expected
- Relative uncertainty is 9%, including uncertainties on all of the input terms
- Uncertainty dominated by the current theory uncertainty on $B(Bc \rightarrow J/\psi \mu^+ \nu_\mu)$ 8.1%
 - Using [this](#) and [this](#) lattice paper for the current estimate along with exclusive $|V_{cb}|$
 - Uncertainty is reducible if decay form factors are measured e.g. in an angular analysis (LHCb and FCC-ee can both do this)
- Signal yield uncertainty from fit is 2.4%, which increases to 3.4% assuming the same level of systematics than statistics
 - Excellent precision using only one tau decay mode!

Sensitivity to New Physics

- Can consider the ratio $R_c = \mathcal{B}(B_c \rightarrow \tau \nu_\tau) / \mathcal{B}(B_c \rightarrow J/\psi \mu^+ \nu_\mu)$ which has 4% precision
 - $|V_{cb}|$ independent, can assume no NP in the muonic mode for theory calculation
- R_c measurement at FCC-ee can strongly constraint both 2HDM and leptoquark parameter space in a complementary manner to other key observables
 - Leptoquark couplings can introduce O(10-100) variations



Detector Considerations for Heavy Flavour



- Limited layouts considered thus far (IDEA, CLD)
 - Designed with higher-energy requirements in mind like Higgs programme
- With 4 IPs under considerations, could diversify the FCC-ee detector attributes
 - A dedicated flavour experiment is possible
 - Design studies are now of high importance
- High-precision vertexing
 - Crucial for modes exploiting $\tau \rightarrow 3\pi\nu_\tau$
 - Lifetime resolution in B0s mixing
- Particle ID
 - K vs π for CP violation studies
 - Hadron rejection in $B0(s) \rightarrow \mu^+\mu^-$
- Calorimetry
 - π^0 reconstruction to surpass LHCb
 - High resolution photons $\tau^+ \rightarrow \mu^+\gamma$

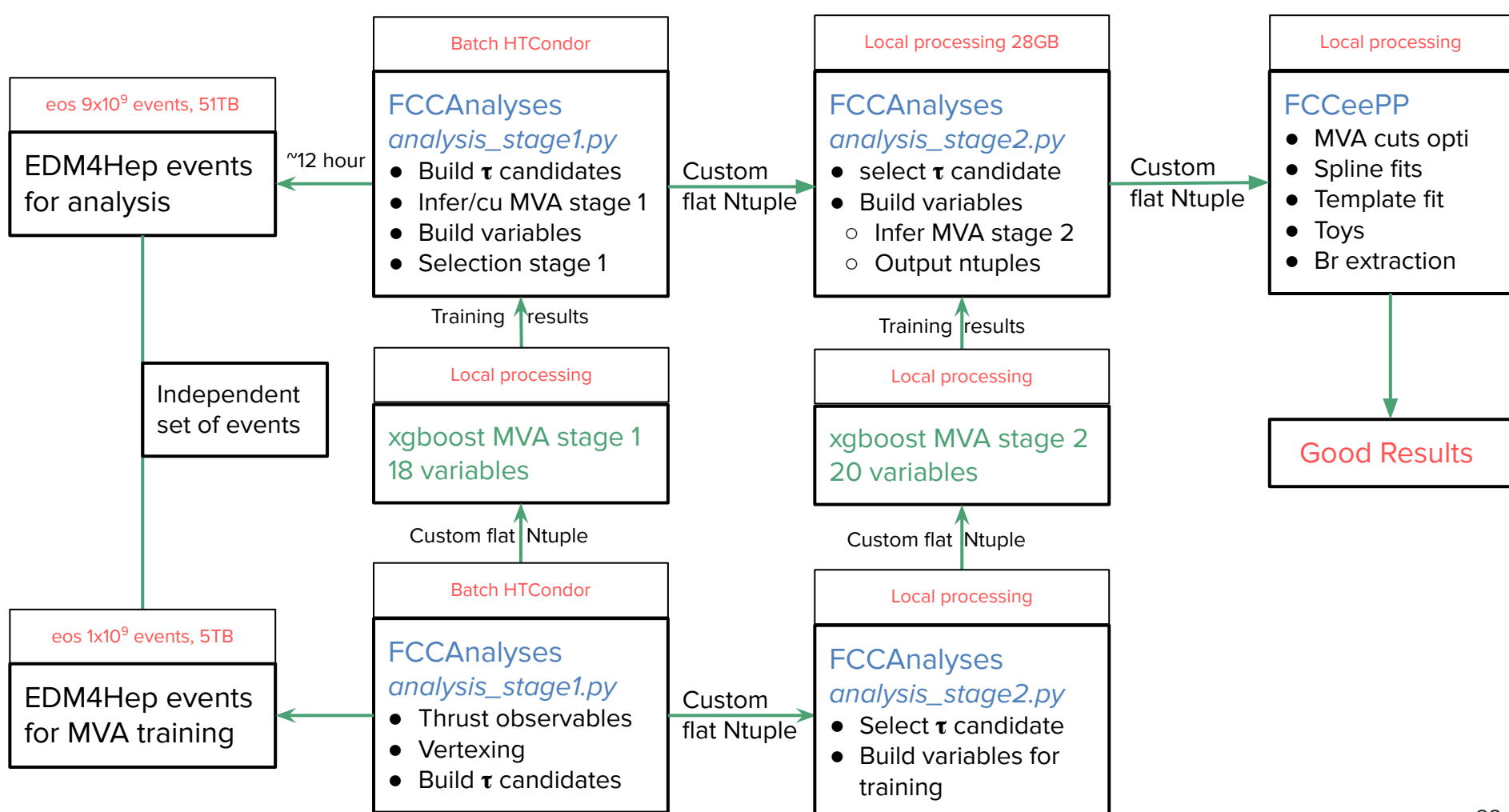
Summary



- The Flavour Physics case is part of the FCC program in its own right
 - There are exciting times ahead with Flavours with the present data and this to come. It can be a lot of fun to think of these perspectives and some serious studies (though part-time !) to be conducted.
- Fantastic tool for Higgs, top, and EWPT tests
 - Unique flagship modes in Flavours have been identified. The core of the program is to be assessed quantitatively. FCC-ee precision shall meet or increase the precision of each and both of Belle II and LHCb upgrades (super-complementarity)
- The project is mature. FCC can be done ! The FCC software and detector full simulations are getting up. Please check:
 - <http://hep-fcc.github.io/FCCSW/>
 - <https://hep-fcc.github.io/FCCeePhysicsPerformance/>

Backup material





Pre-selection before first-stage MVA

- The following cuts are applied prior to first-stage MVA training
 - A primary vertex is reconstructed
 - At least one reconstructed 3π candidate in the event
 - One of the 3π candidate must be in the lower energy hemisphere

- These pre-selection cuts are applied to signal and inclusive $Z \rightarrow bb/cc/qq$ background samples

First-stage MVA



- Strategy

- Train on general event-level properties, harnessing difference in hemisphere energies between $Bc^+ \rightarrow \tau^+ \nu_\tau$ and $Z \rightarrow bb/cc/qq$
- Also use information on PV multiplicity, number of vertices reconstructed in event, number of 3π candidates, and distance between decay vertices and PV
- Background training sample is a mix of inclusive $Z \rightarrow bb/cc/qq$, combined according to Z branching ratios and efficiency of pre-selection requirements

Selection cuts before second-stage MVA



- Apply $MVA_1 > 0.6$ cut to remove “easy” stuff
- Select the reconstructed 3π candidate with the smallest displaced vertex χ^2
- Selected vertex must be in the hemisphere with less energy
- Apply $m(\pi\pi)$ cuts to 3π candidates to select $\rho \rightarrow \pi^+\pi^-$ region [0.6, 1] GeV
 - Signal decays purely via $\tau \rightarrow a_1 \rightarrow \rho\pi$ resonance
- Require $m(3\pi) < m_\tau$, and that the difference in hemisphere energy exceeds 10 GeV

Second-stage MVA



- Strategy:

- Trained on signal and inclusive background passing pre-selection (previous slide)
- Use properties of 3π candidate (mass, momentum, IP, distance from PV, angle of momentum to thrust axis)
- Use IP to the PV for other decay vertices in the event. Associated charm hadron produced with $B_c^+ \rightarrow \tau^+ \nu_\tau$ originates from PV, unlike the charm hadron in $B^0 \rightarrow D^{(*)} \tau^+ \nu_\tau$
- Mass of PV - this is larger for background because the associated charm hadron in $B_c^+ \rightarrow \tau^+ \nu_\tau$ carries energy away from the PV
- Nominal B energy = $m(Z)$ - sum of all reconstructed event energy apart from $E(3\pi)$

First stage MVA variables

The BDT is trained using the following features:

- Total reconstructed energy in each hemisphere;
- Total charged and neutral reconstructed energies in each hemisphere;
- Charged and neutral particle multiplicities in each hemisphere;
- Number of tracks in the reconstructed PV;
- Number of reconstructed 3π candidates in the event;
- Number of reconstructed vertices in each hemisphere;
- Minimum, maximum, and average radial distance of all decay vertices from the PV.

First stage MVA

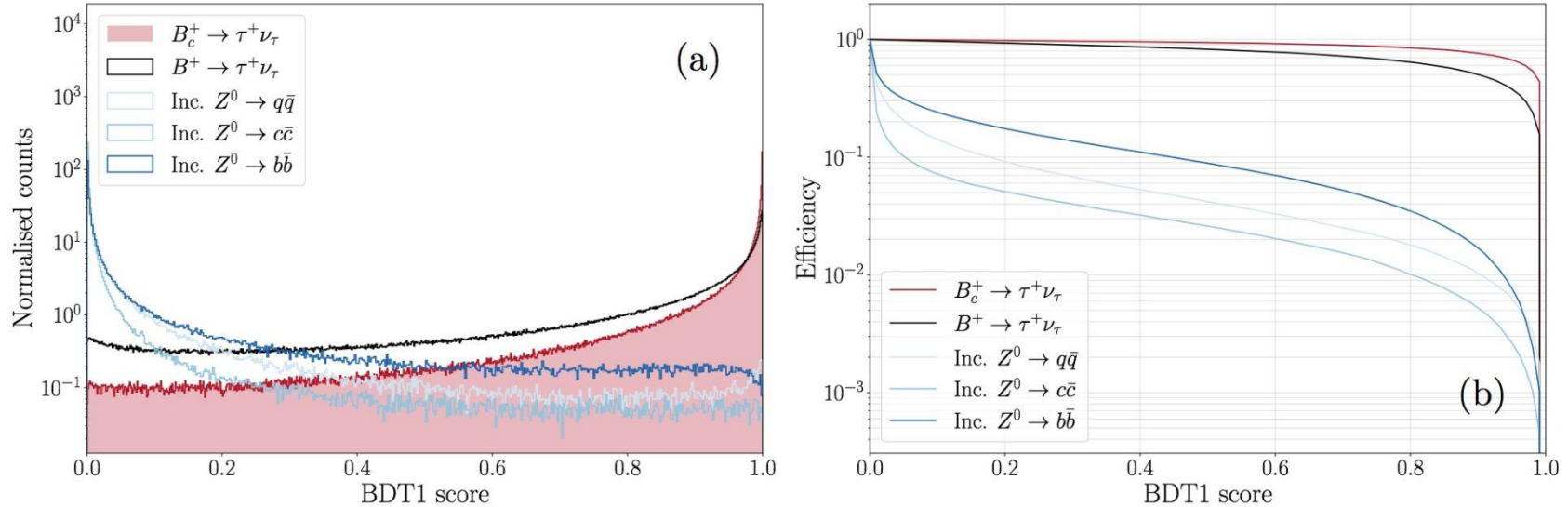


Figure 2: (a) First-stage BDT distribution in signal, $B^+ \rightarrow \tau^+ \nu_\tau$ background, and inclusive Z background. (b) Efficiency of the first-stage BDT as a function of cut value.

Second stage MVA variables

The BDT is trained on the following features:

- 3π candidate mass, and masses of the two $\pi^+\pi^-$ combinations;
- Number of 3π candidates in the event;
- Radial distance of the 3π candidate from the PV;
- Vertex χ^2 of the 3π candidate;
- Momentum magnitude, momentum components, and impact parameter (transverse and longitudinal) of the 3π candidate;
- Angle between the 3π candidate and the thrust axis;
- Minimum, maximum, and average impact parameter (longitudinal and transverse) of all other reconstructed decay vertices in the event;
- Mass of the PV;
- Nominal B energy, defined as the Z mass minus all reconstructed energy apart from the 3π candidate.

Second stage MVA

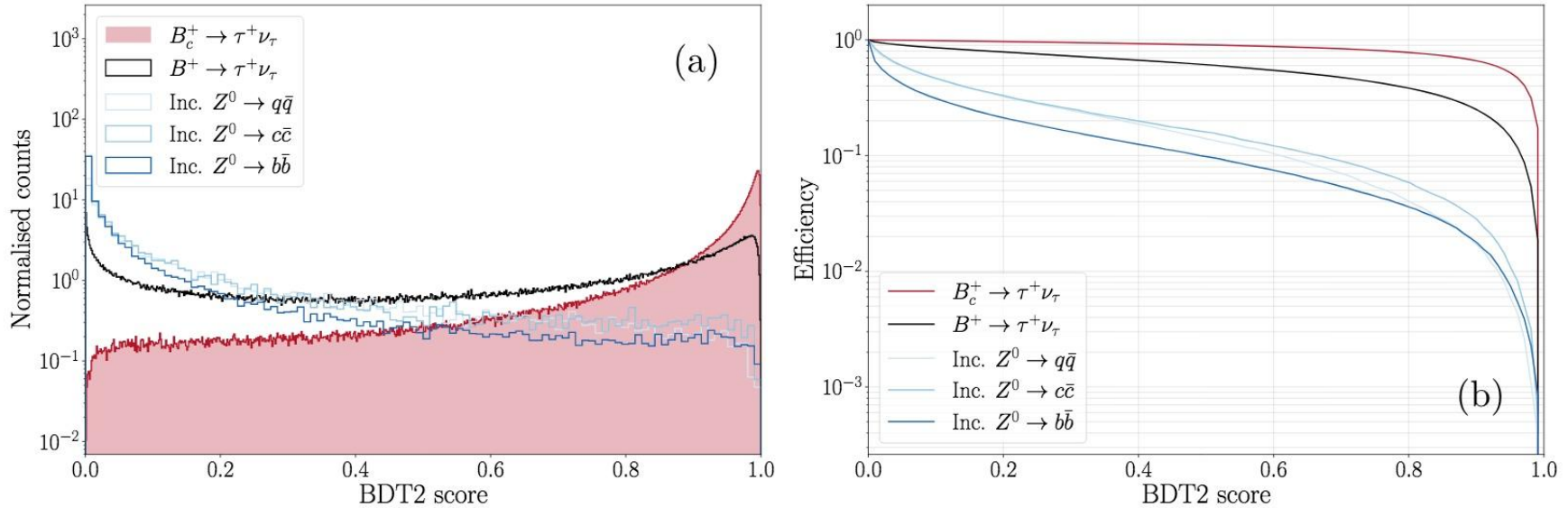


Figure 3: (Left) Second-stage BDT distribution in signal, $B^+ \rightarrow \tau^+ \nu_\tau$ background, and inclusive Z background. (Right) Efficiency of the second-stage BDT as a function of cut value.

Background composition

Prior to the BDT cut optimisation, none of the 10^9 inclusive $Z \rightarrow c\bar{c}$ and $Z \rightarrow q\bar{q}$ events are found to pass sufficiently tight cuts on both BDTs. As such, background from these sources is not considered in the optimisation or subsequent fit studies. After the same cuts, the remaining statistics in the inclusive $Z \rightarrow b\bar{b}$ sample are found to be insufficient for determining the background rejection accurately in the cut optimisation. To boost the background statistics for the optimisation, samples of exclusive b -hadron decays are generated, where the decay modes are chosen based on the composition of the remaining inclusive $Z \rightarrow b\bar{b}$ sample. The following decays are considered:

where $B \in \{B^0, B^+, B_s^0, \Lambda_b^0\}$ and the corresponding $D \in \{D^-, \bar{D}^0, D_s^-, \Lambda_c^-\}$. In each of the exclusive b -hadron samples, all of the b -hadron decay products are decayed inclusively. The list of exclusive decays considered is not exhaustive, and covers around 10% of the decay width for each B hadron. As a result, a factor 2.5 difference in rate relative to the inclusive $Z \rightarrow b\bar{b}$ sample is observed after tight BDT cuts. This factor is used to scale the exclusive sample yield estimates in the optimisation procedure, in order to avoid underestimating the expected background level.

- $B \rightarrow D\tau^+\nu_\tau$
- $B \rightarrow D^*\tau^+\nu_\tau$
- $B \rightarrow D\pi^+\pi^+\pi^-$
- $B \rightarrow D^*\pi^+\pi^+\pi^-$
- $B \rightarrow DD_s^+$
- $B \rightarrow D^*D_s^+$
- $B \rightarrow D^*D_s^{*+}$

Background estimation

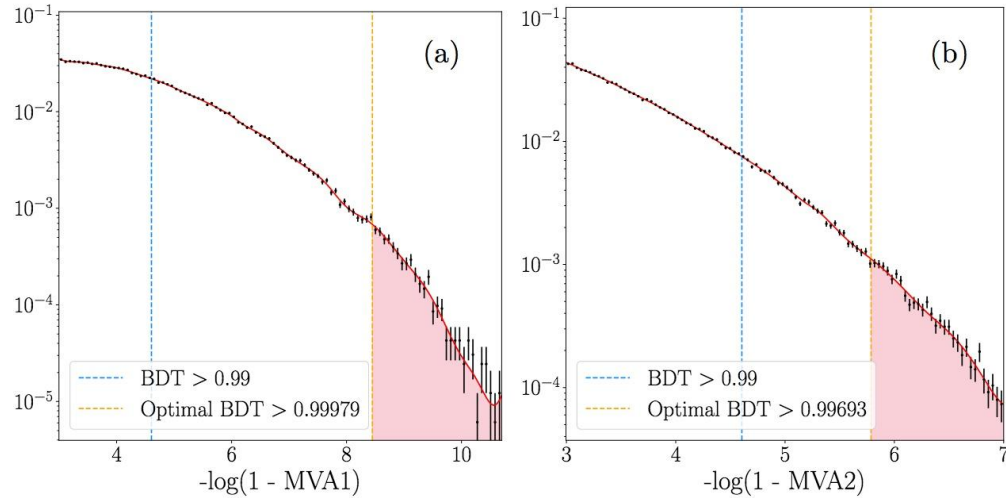


Figure 4: (a) BDT1 distribution above 0.95 for a combined sample of exclusive b -hadron decays. (b) BDT1 distribution above 0.95 for a combined sample of exclusive b -hadron decays. The cubic spline parameterisations are shown by solid red lines, example cuts of $\text{BDT} > 0.99$ by the dashed blue lines, and the optimal BDT cuts by the dashed orange lines. The background efficiency given prior cuts of > 0.95 on both BDTs is given by the product of the spline integrals above the optimal cuts (red areas), where each integral is normalised to the respective spline integral across the full range.

Discriminating variable

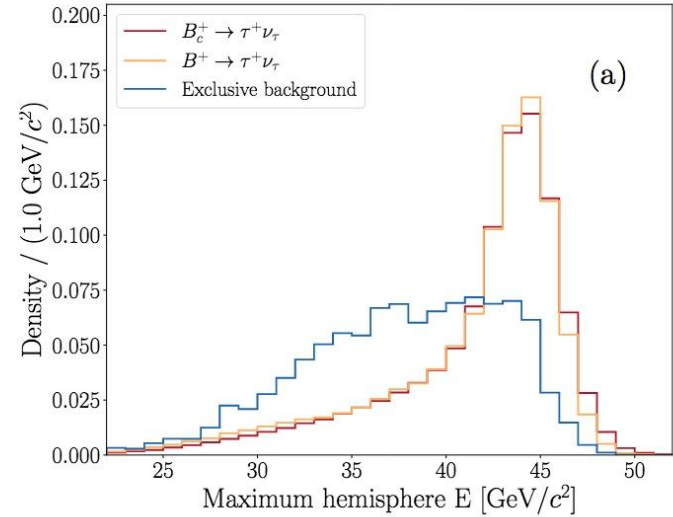
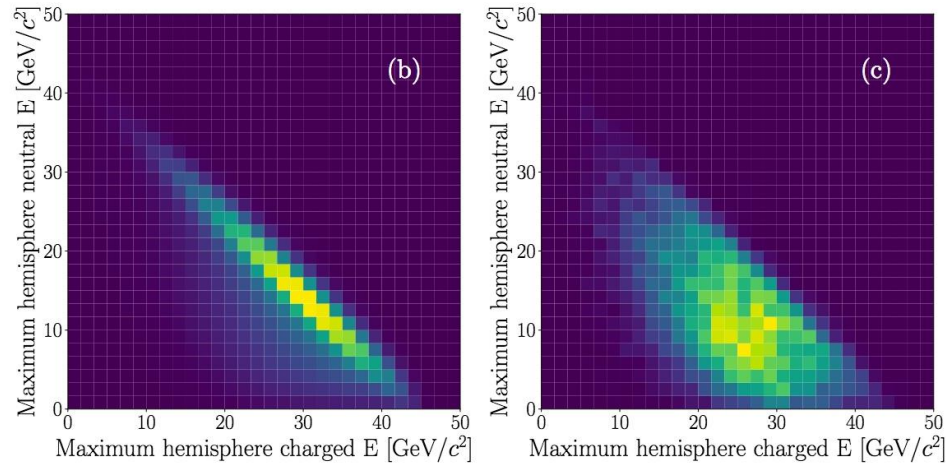


Figure 5: (a) Distribution of total hemisphere energy for the maximum energy hemisphere. Signal and $B^+ \rightarrow \tau^+ \nu_\tau$ decays closely follow the expected distribution for an inclusive b -quark decay from a Z , whereas the background distribution is biased downwards by the selection. (b/c) Relationship between the total charged and neutral energy in the maximum energy hemisphere for $B_c^+ \rightarrow \tau^+ \nu_\tau$ / inclusive $Z \rightarrow b\bar{b}$ events.

Fit

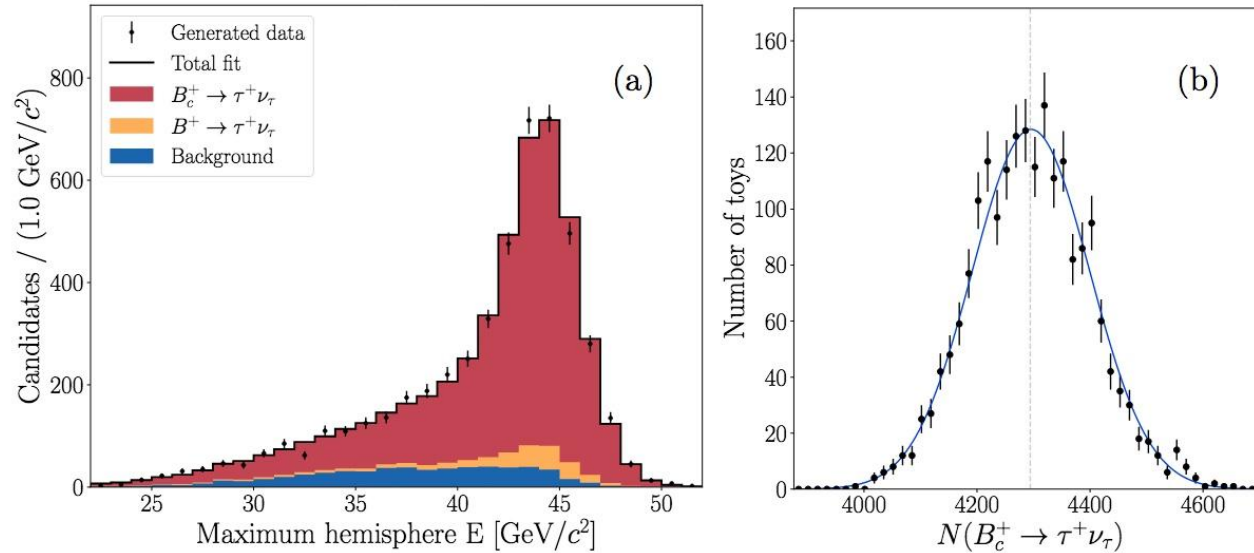


Figure 6: (a) Result of a single pseudoexperiment fit, where the peaking signal is clearly distinguishable from the background. (b) Signal yields measured in 2000 pseudoexperiment fits, where the generated value is indicated by the dashed vertical line.

Bc- \rightarrow Tau nu Yields

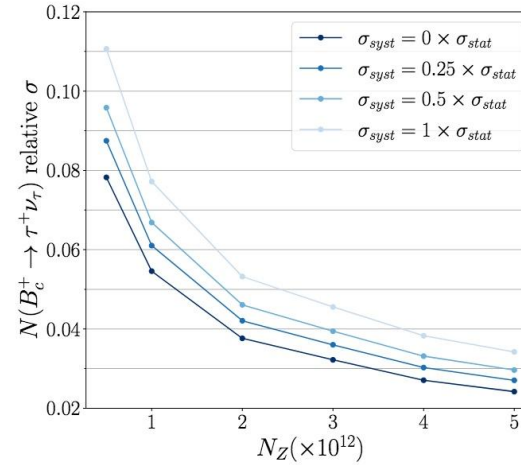


Figure 7: Relative precision on the signal yield as a function of N_Z . The signal yields at each N_Z value are taken from the cut optimisation procedure, and the statistical uncertainties are measured in pseudoexperiment fits. Different levels of systematic uncertainty relative to the statistical uncertainty are also shown.

$N_Z (\times 10^{12})$	$N(B_c^+ \rightarrow \tau^+ \nu_\tau)$	Relative σ (%)
0.5	430 \pm 33	7.8
1	858 \pm 46	5.5
2	1717 \pm 64	3.8
3	2578 \pm 83	3.2
4	3436 \pm 93	2.7
5	4295 \pm 103	2.4

Table 1: Estimated signal yields as a function of N_Z , where the uncertainties quoted are statistical only. The yield central values are determined from the cut optimisation procedure, and the uncertainties from pseudoexperiment fits.

Towards Branching Fraction

With $B_c^+ \rightarrow J/\psi \mu^+ \nu_\mu$ as a normalisation mode, the ratio of branching fractions

$$\begin{aligned} R_c &= \frac{\mathcal{B}(B_c^+ \rightarrow \tau^+ \nu_\tau)}{\mathcal{B}(B_c^+ \rightarrow J/\psi \mu^+ \nu_\mu)} \\ &= \frac{N(B_c^+ \rightarrow \tau^+ \nu_\tau)}{N(B_c^+ \rightarrow J/\psi \mu^+ \nu_\mu)} \times \frac{\epsilon(B_c^+ \rightarrow J/\psi \mu^+ \nu_\mu)}{\epsilon(B_c^+ \rightarrow \tau^+ \nu_\tau)} \times \frac{\mathcal{B}(J/\psi \rightarrow \mu^+ \mu^-)}{\mathcal{B}(\tau^+ \rightarrow \pi^+ \pi^+ \pi^- \bar{\nu}_\tau)} \end{aligned}$$

It is also possible to determine an absolute branching fraction for the signal decay,

$$\mathcal{B}(B_c^+ \rightarrow \tau^+ \nu_\tau) = R_c \times \mathcal{B}(B_c^+ \rightarrow J/\psi \mu^+ \nu_\mu)^{\text{SM}},$$

Results

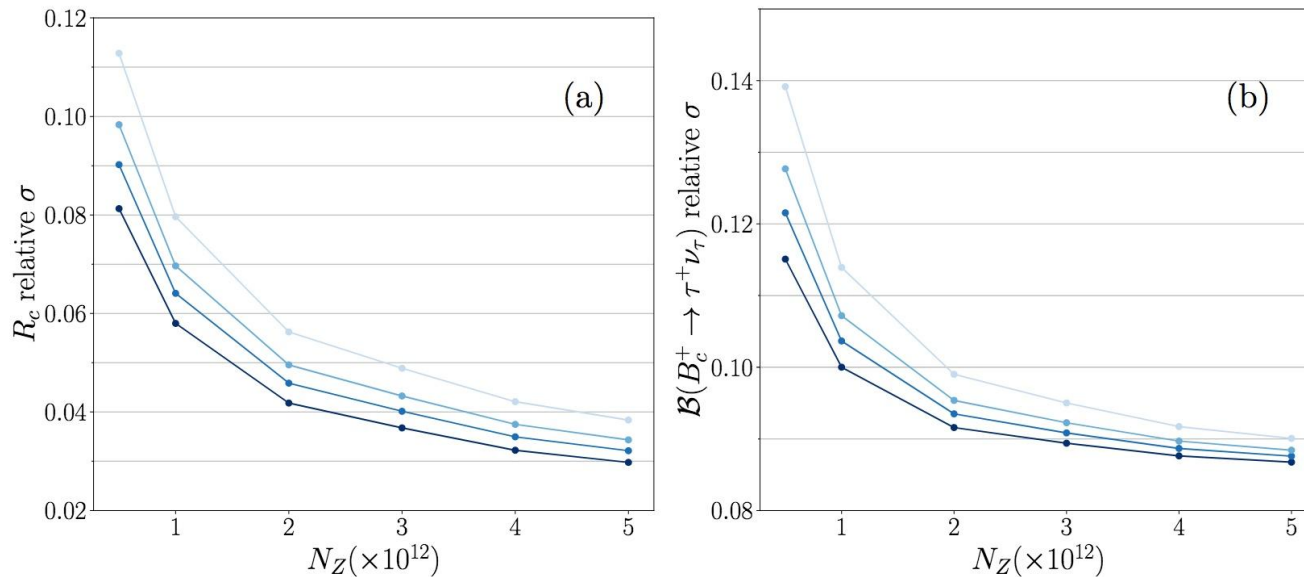


Figure 8: (a) Relative precision on the ratio of branching fractions $R = \mathcal{B}(B_c^+ \rightarrow \tau^+ \nu_\tau) / \mathcal{B}(B_c^+ \rightarrow J/\psi \mu^+ \nu_\mu)$ as a function of N_Z . (b) Relative precision on $\mathcal{B}(B_c^+ \rightarrow \tau^+ \nu_\tau)$ as a function of N_Z , using a SM prediction for $\mathcal{B}(B_c^+ \rightarrow J/\psi \mu^+ \nu_\mu)$. The different shades of blue correspond to different levels of systematic uncertainty on $N(B_c^+ \rightarrow \tau^+ \nu_\tau)$ relative to the statistical uncertainty, following the same colour scheme as Fig. 7.

New physics - 2HDM

Thanks to Olcyr Sumensari for the interpretation work, which is based on the analysis precision estimates

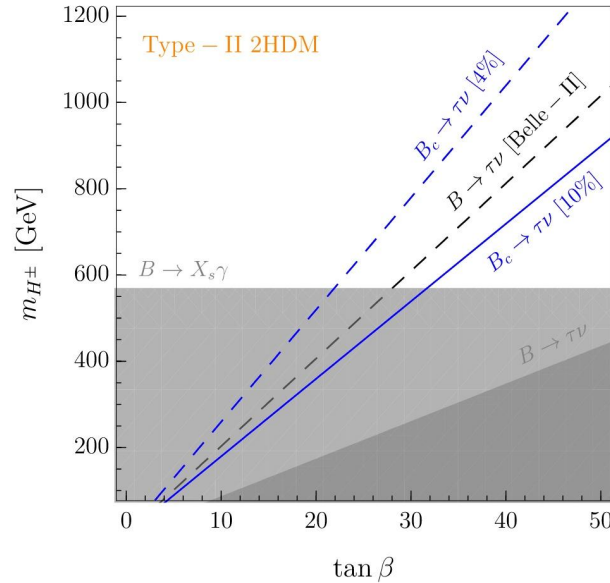


Figure 9: Expected constraints on the plane $\tan \beta$ vs. m_{H^\pm} for type-II 2HDM derived by assuming a relative uncertainty on $\Gamma(B_c^+ \rightarrow \tau^+ \nu_\tau)/|V_{cb}|^2$ of 10% (solid blue line) and 4% (dashed blue line). Current constraints obtained from $\mathcal{B}(B \rightarrow X_s \gamma)$ [64] and $\mathcal{B}(B^+ \rightarrow \tau^+ \nu_\tau)$ [61] are depicted by the grey regions. Prospects for a $\mathcal{B}(B^+ \rightarrow \tau^+ \nu_\tau)$ measurement at Belle-II are depicted by the grey dashed line, obtained under the assumption of 5% uncertainty on the branching fraction [69].

New physics - Leptoquarks

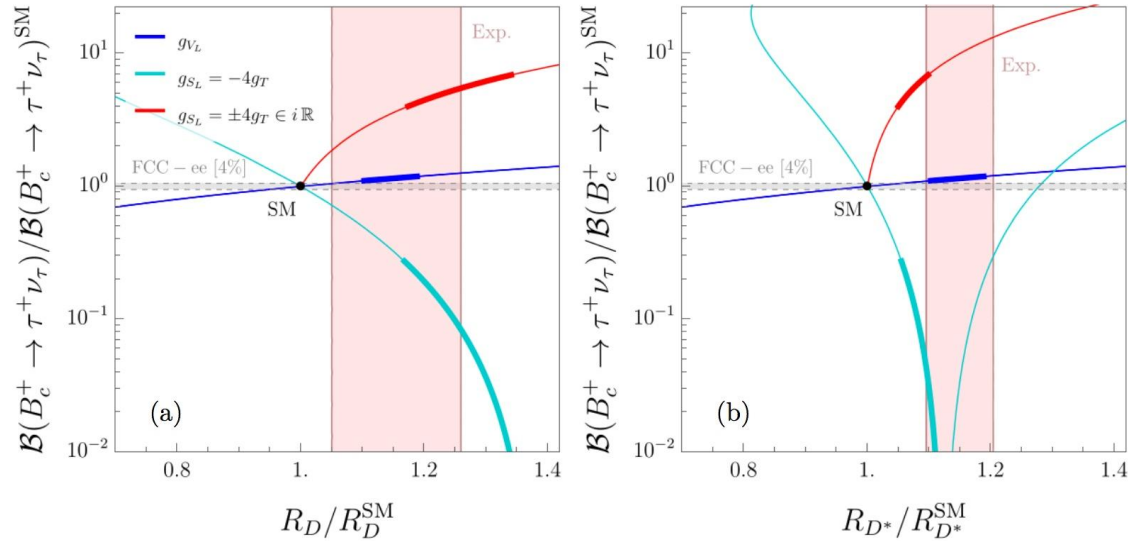


Figure 10: Predictions for (a) R_D/R_D^{SM} and (b) $R_{D^*}/R_{D^*}^{\text{SM}}$ are plotted against the ratio $\mathcal{B}(B_c^+ \rightarrow \tau^+ \nu_\tau) / \mathcal{B}(B_c^+ \rightarrow \tau^+ \nu_\tau)^{\text{SM}}$ in several effective scenarios: (i) g_{V_L} (blue), (ii) $g_{S_L} = -4g_T$ (cyan), and (iii) $g_{S_L} = +4g_T \in i\mathbb{R}$ (red), which are defined at $\Lambda \approx 1$ TeV. The thick lines correspond to the values of the effective couplings favoured by the current fit to $b \rightarrow c\tau\nu_\tau$ data [71]. The red shaded regions denote the current experimental averages of R_D and R_{D^*} at 1σ accuracy [23]. The grey region corresponds to the estimated sensitivity of 4% precision on $\Gamma(B_c^+ \tau^+ \nu_\tau) / |V_{cb}|^2$ at FCC-ee.

Summary

The sensitivities for both the branching fraction of $B_c^+ \rightarrow \tau^+ \nu_\tau$ and the ratio $R_c = \mathcal{B}(B_c^+ \rightarrow \tau^+ \nu_\tau) / \mathcal{B}(B_c^+ \rightarrow J/\psi \mu^+ \nu_\mu)$ are estimated as a function of the number of collected Z decays, where a relative precision of around 4% is achieved for R_c with $N_Z = 5 \times 10^{12}$. The precision on the absolute branching fraction is limited to around 8% due to knowledge of the $B_c^+ \rightarrow J/\psi \mu^+ \nu_\mu$ decay form factors, which can be improved through dedicated measurements of this mode in future.

The impact of a measurement of $B_c^+ \rightarrow \tau^+ \nu_\tau$ on NP scenarios is also discussed. In particular, it is shown that such a measurement at FCC-ee can constrain a large region of the $(\tan \beta, m_{H^\pm})$ plane in the type-II 2HDM, which cannot be covered by other flavour-physics measurements. Recently, leptoquark models have received significant attention as the only viable explanation of the B -physics anomalies in both charged and neutral current processes. A precise measurement of the branching fraction of $B_c^+ \rightarrow \tau^+ \nu_\tau$ at FCC-ee could fully probe the interpretations of R_D and R_{D^*} that are permitted under existing constraints.

In summary, this work demonstrates why FCC-ee is the most well-suited environment for a measurement of the branching fraction of the $B_c^+ \rightarrow \tau^+ \nu_\tau$ decay, and represents the first FCC-ee analysis to use common software tools from EDM4HEP through to final analysis.